Structure and scattering in colloidal ferrofluids

Philip J. Camp and G. N. Patey
Department of Chemistry, University of British Columbia, Vancouver, British Columbia, Canada V6T 1Z1
(Received 22 May 2000)

The structure of a model colloidal ferrofluid, the dipolar hard-sphere fluid, at low temperature has been investigated using Monte Carlo simulations. Extensive particle association into chainlike and ringlike clusters is observed at low density. The structure factors have been calculated, and are analyzed with the aid of simple scaling arguments. We describe the progression of fluid structures from the low-density associated phase, to the high-density liquid phase. This paper may be of help in obtaining an experimental observation of a fluid-fluid transition in colloidal ferrofluids.

PACS number(s): 61.20.Ja, 61.20.Qg, 61.25.Em, 25.40.Dn

I. INTRODUCTION

Colloidal ferrofluids have received a great deal of attention over the last four decades, not least because of the utility of such materials in modern technological applications. Ferrofluids are typically suspensions of roughly spherical ferromagnetic particles coated with a thin layer of inert nonmagnetic material that protects the system from irreversible aggregation. The dominant interactions are those between the magnetic dipoles; the short-range van der Waals attractions between the coatings are relatively weak, and hence only provide a slight sticking effect when two particles come close to contact. One of the earliest experimental observations of ferrofluid structure was due to Hess and Parker [1], who studied colloidal cobalt particles with a variety of polymer coatings. They obtained electron photomicrographs of low-density colloids, in the absence of a magnetic field, which showed a highly associated structure provided the magnetization of the magnetic material was large enough.

Early experimental studies such as this stimulated theoretical investigations of association phenomena in colloidal ferrofluids by de Gennes and Pincus [2], and later by Jordan [3]. In these works the ferrofluid is modeled as a monodisperse fluid of hard spheres of diameter σ, carrying central point dipoles of magnitude μ. The pair interaction, $u(1,2)$, in the dipolar hard sphere (DHS) model is given by

$$u(1,2)=u_{\mathrm{HS}}(r)-\frac{\mu^2}{r^3}[3(\hat{\boldsymbol{\mu}}_1\cdot\hat{\mathbf{r}})(\hat{\boldsymbol{\mu}}_2\cdot\hat{\mathbf{r}})-\hat{\boldsymbol{\mu}}_1\cdot\hat{\boldsymbol{\mu}}_2], \quad (1)$$

where $u_{\mathrm{HS}}(r)$ is the hard-sphere interaction, μ is the dipole moment, $\hat{\boldsymbol{\mu}}_j$ is a unit vector along the dipole of particle j, $\hat{\mathbf{r}}$ is a unit vector along the interparticle vector $\mathbf{r}$, and $r=|\mathbf{r}|$. The potential clearly favors a parallel nose-to-tail arrangement, and is therefore responsible for the stability of highly associated structures at low temperatures. In the following it will prove useful to define the reduced temperature $T^*=k_{\mathrm{B}}T\sigma^3/\mu^2$, the reduced reciprocal temperature $\beta^*=1/T^*$, the reduced dipole moment $\mu^*=\sqrt{\beta^*}$, and the reduced number density $\rho^*=N\sigma^3/V$, where k_{B} is Boltzmann's constant, N is the number of particles, and V is the volume. For spherical, single-domain ferromagnetic particles the dipole moment is $\pi\sigma^3M/6$, where M is the magnetization. In typical colloidal ferrofluids $\sigma\sim100$ Å, and $M\sim1000$ Oe, which at room temperature leads to T^* in the range 0.1–1. We note, however, that in Ref. [1], a highly chained structure was observed in a sample with $T^*\simeq0.02$.

In Ref. [2], de Gennes and Pincus studied the pair correlations in the DHS fluid, which provided some explanation as to how associated structures can arise. In particular, they argued that at low densities and temperatures, in zero magnetic field, chainlike and ringlike clusters can coexist. Rings are the ground-state structure for clusters of $n\geqslant4$ dipolar spheres [4–7]. Most subsequent theoretical treatments of particle association in the DHS fluid have relied on an asymptotic evaluation of the partition function of a single pair of particles [8–10] to estimate the thermodynamics of chains, similar in spirit to the original works of de Gennes and Pincus [2], and Jordan [3]. This is a severe oversimplification, because the long-range nature of the dipole-dipole potential demands that three-body and higher correlations be significant at low temperatures. It is hard to imagine how an accurate theoretical treatment of such strongly interacting dipolar particles can be made tractable.

The first computer-simulation studies of particle association in DHS fluids were by Weis and Levesque [11,12]. In the first of their papers [11], they report extensive particle association in Monte Carlo (MC) simulations of, typically, $N=500$ particles at densities in the range $0.05\leqslant\rho^*\leqslant0.2$ and temperatures $T^*\leqslant0.16$. Chains were identified using an energy-based criterion that reflects the close proximity and near-parallel alignment of neighboring particles in a cluster [13]. The mean number of spheres per chain varied from about 7 at $(\rho^*=0.1,T^*=0.16)$, up to about 30 at $(\rho^*=0.05,T^*=0.0816)$. By drawing an analogy between chains and polymers, a persistence length can be defined, which is the correlation length of the unit dipole vectors along the chain; it is the distance over which the chain is effectively linear. In chains consisting of at least ten spheres, this length varied between 4σ and 9σ, depending on density and temperature. Typical simulation configurations showed many chainlike clusters, with rings being observed only rarely at the densities considered, and the structure factor exhibited a low wave vector peak due to particle association. The chains were observed to break, and recombine, by which a given particle could migrate from one chain to another. However,

the question of convergence was raised in the simulations at low density and temperature, in which the mean chain length was seen to increase slowly over the course of runs consisting of up to 3×10^5 attempted moves per particle, even though the energy remained fairly constant.

A surprising result from the work of Weis and Levesque was that no vapor-liquid transition was in evidence. Condensation was also absent in the simulations of the DHS fluid by Caillol [14], and in simulations of a related model, the Stockmayer fluid, by van Leeuwen and Smit [15]. Recently, however, we have presented three completely independent sets of simulation evidence that all point to the existence of a condensation transition in the DHS fluid [16]. The transition occurs between a highly associated vapor phase, and a more normal dense liquid phase, with extremely small changes in enthalpy and entropy. Rough estimates for the critical parameters are $T_c^*\simeq0.16$, and $\rho_c^*\simeq0.1$. We stress that these results are *not* relevant to colloidal ferrofluids in aqueous salt solutions. In these so-called ionic ferrofluids, the vapor-liquid transition is driven by screened electrostatic, and van der Waals interactions (see, e.g., Refs. [17] and [18]).

At high densities, dipolar fluids can exhibit orientational order with a net dipole moment. The so-called ferroelectric phase was observed in the dipolar soft-sphere (DSS) fluid by Wei and Patey [19,20], and in the DHS fluid by Weis and Levesque [11,12,21]. The behavior of the DSS fluid as a function of density and applied field was examined by Stevens and Grest [22], who observed an equilibrium mixture of chainlike and ringlike clusters at low temperature and density. Recently, the effect of size and dipole-moment polydispersities on particle association and orientational order in DHS fluids has been considered by Costa Cabral [23].

In this paper we revisit the low-temperature DHS fluid using constant-volume MC simulations. In the light of recent evidence for the existence of a vapor-liquid transition, we investigate the structural properties of the fluid at low temperature, as a function of density. One of our aims is to present accurate results for the structure factor in the region of the phase transition. This affords insight into the evolution of the structure, from the low-density vapor phase to the dense liquid phase. It also provides some indication of what should be observed in scattering experiments on the different isotropic fluid phases of real colloidal ferrofluids. This is particularly important if the vapor-liquid transition is to be observed in the laboratory. For the most part our simulations employed 256 particles, which meant that we were able to perform simulations up to two orders of magnitude longer than those of Weis and Levesque. We have performed a check with a well-equilibrated system of 512 particles at a single density and temperature, which showed identical results to the corresponding 256-particle system. Therefore, we are confident that our simulations provide an accurate representation of the structure and scattering in colloidal ferrofluids. In Sec. II we provide details of the simulation method. The results are presented in Sec. III, and Sec. IV concludes the paper.

II. COMPUTER SIMULATIONS

MC simulations [24] were performed with a fixed number of particles, $N=256$, in a volume V, and at temperature T. The simulation cell was cubic, of side L, and periodic boundary conditions were applied. The long-range dipole-dipole interactions were handled using the Ewald summation method [24,25], with conducting boundary conditions ($\epsilon'=\infty$). On average, one MC sweep consisted of one attempted translation and rotation per particle. Maximum displacement parameters were adjusted to give an acceptance rate of about 50%.

Simulations were performed along a single isotherm, $T^*=0.1\dot{3}$ ($\beta^*=7.5,\mu^*\simeq2.74$), which, according to the data from Ref. [16], is below the critical temperature ($T_c^*\simeq0.16$). The densities simulated were $\rho^*=0.001$, $\rho^*=0.005$, $\rho^*=0.01$, $\rho^*=0.06$, $\rho^*=0.17$, $\rho^*=0.35$, $\rho^*=0.5$, and $\rho^*=0.6$; the vapor-liquid transition at $T^*=0.1\dot{3}$ lies in the range $\rho^*=0.06$–0.35 [16]. The simulations converged very slowly, especially at the lowest densities; equilibration required up to $\mathcal{O}(10^7)$ MC sweeps, while the production runs consisted of at least 2×10^6 MC sweeps. Averages were accumulated over blocks of 10^3 MC sweeps, and statistical uncertainties were calculated by assuming that the block averages were statistically independent.

The structure factor was calculated by explicit evaluation of the expression [26]

$$S(\mathbf{q})=\frac{1}{N}\left\langle\sum_{j=1}^{N}\sum_{k=1}^{N}\exp[i\mathbf{q}\cdot(\mathbf{r}_j-\mathbf{r}_k)]\right\rangle,$$
$$=\frac{1}{N}\left\langle\left(\sum_{j=1}^{N}\cos\mathbf{q}\cdot\mathbf{r}_j\right)^2+\left(\sum_{j=1}^{N}\sin\mathbf{q}\cdot\mathbf{r}_j\right)^2\right\rangle. \quad (2)$$

The wave vectors, $\mathbf{q}$, were commensurate with the periodic boundary conditions, i.e., $\mathbf{q}=(2\pi/L)(l,m,n)\neq(0,0,0)$, where l, m, and n are integers such that $\sqrt{l^2+m^2+n^2}\leqslant30$; $S(\mathbf{q})$ was thus evaluated for wave vectors with magnitudes in the range $2\pi/L\leqslant|\mathbf{q}|\leqslant60\pi/L$. Since the fluid structure is expected to be translationally invariant, $S(q)$ is obtained by averaging the contributions from all wave vectors of magnitude $|\mathbf{q}|=q$.

Orientational order was monitored by calculating the second-rank order tensor, $\mathbf{Q}$, defined by [27]

$$\mathbf{Q}=\frac{1}{2N}\sum_{j=1}^{N}(3\hat{\boldsymbol{\mu}}_j\hat{\boldsymbol{\mu}}_j-\mathbf{I}), \quad (3)$$

where $\mathbf{I}$ is the second-rank unit tensor. Diagonalization of $\mathbf{Q}$ yields three eigenvalues and three eigenvectors. The highest eigenvalue is the second-rank order parameter, P_2, and the corresponding unit eigenvector is the director, $\hat{\mathbf{n}}$ [28]. P_2 can also be expressed as the average of $(3\cos^2\theta-1)/2$ over all of the particles, where θ is the angle between the orientation vector of a given particle and the instantaneous director. P_2 is unity in a perfectly aligned ferroelectric phase, and zero in an isotropic phase. The polarization P_1 is given by

$$P_1=\left|\frac{1}{N}\sum_{j=1}^{N}\hat{\boldsymbol{\mu}}_j\cdot\hat{\mathbf{n}}\right|. \quad (4)$$

P_1 is unity in a perfectly aligned ferroelectric phase and zero in an isotropic phase. Finite-size effects are apparent in

TABLE I. *NVT*-MC simulation results for the DHS fluid along the isotherm $T^*=0.1\dot{3}$. ρ^* is the reduced number density, U is the configurational energy, P_1 is the polarization, and P_2 is the nematic order parameter. A and D are the fit parameters to $S(q)=A(q\sigma)^{-D}$ in the range $1\leqslant q\sigma\leqslant\pi$. The figures in parentheses represent the statistical uncertainty in the last digit.

N	ρ^*	U/Nk_BT	P_1	P_2	A	D
256	0.001	−12.7(1)	0.02(1)	0.07(2)	3.33(1)	1.25(1)
256	0.005	−13.6(1)	0.05(3)	0.08(3)	3.03(2)	1.07(1)
256	0.01	−14.1(1)	0.13(4)	0.10(3)	2.89(3)	0.98(1)
512	0.01	−14.09(6)	0.03(1)	0.07(1)	2.93(4)	0.99(2)
256	0.06	−14.5(1)	0.08(3)	0.09(3)	2.75(5)	0.96(3)
256	0.17	−14.5(1)	0.11(6)	0.10(3)	1.83(4)	0.69(3)
256	0.35	−14.5(1)	0.2(1)	0.11(4)		
256	0.5	−14.6(1)	0.4(1)	0.14(5)		
256	0.6	−15.0(1)	0.65(8)	0.32(8)		

P_2 calculated via the diagonalization of $\mathbf{Q}$ [29]; in the isotropic fluid the errors are $\mathcal{O}(1/\sqrt{N})$, while in orientationally ordered phases they are $\mathcal{O}(1/N)$.

III. RESULTS

The results of the *NVT*-MC simulations along the isotherm $T^*=0.1\dot{3}$ are summarized in Table I. The energy decreases with increasing density up to $\rho^*=0.06$, while in the density range $0.06\leqslant\rho^*\leqslant0.35$ the energy is effectively constant. The remarkably low energy of the very dilute fluid is due to extensive particle association, while the energy is maintained at intermediate densities by the increase in the average coordination number. The subtle changes in energy and entropy accompanying the liquid-vapor phase transition in the range $0.06\leqslant\rho^*\leqslant0.35$ were discussed in Ref. [16]. The fluid exhibits ferroelectric order, as evidenced by P_1 and P_2, at densities above $\rho^*=0.5$, accompanied by an energy change of about $-0.5k_BT$ from the isotropic liquid. This density is to be compared with $\rho^*=0.7$, above which ferroelectric ordering occurs along the isotherm $T^*=0.16$ [12,21]. At high densities the orientationally ordered liquid is stabilized by a subtle balance between short-range interactions and long-range reaction-field effects [19,20,30,31].

In Fig. 1 we show some typical configurations from the simulations at the six lowest densities, i.e., densities in the range $0.001\leqslant\rho^*\leqslant0.35$. We show the two-dimensional projection of the simulation cell and the adjoining halves of the surrounding periodic images; this captures any clusters that straddle the boundary of the central simulation cell.

Figure 1(a) shows a configuration with $\rho^*=0.001$. As predicted by de Gennes and Pincus [2], the fluid consists of a distribution of ringlike clusters coexisting with short chainlike segments, and some free particles. We note that similar configurations were found in simulations of the dipolar soft sphere fluid by Stevens and Grest—see Fig. 2 of Ref. [22]. An important point to note is that the clusters are separated from one another by distances longer than their characteristic dimensions. The implication is that most of the configurational energy arises from intracluster interactions, rather than intercluster interactions, i.e., the low energy of the dilute fluid is due to particle association.

A configuration with density $\rho^*=0.005$ is shown in Fig. 1(b). It is apparent that the average size of the clusters has risen considerably, as well as the proportion of particles in chainlike clusters. The typical size of the chains has increased to such an extent that it is now comparable to the dimensions of the simulation cell.

Figure 1(c) shows that a similar structure occurs at a density $\rho^*=0.01$; very long chainlike clusters coexist with distinct ringlike clusters. One concern regarding the finite size of the simulation cell is that the periodic boundary conditions might artificially stabilize chainlike structures that can span the entire box length; if a single linear chain spans the simulation cell, the energy per particle calculated via the Ewald summation method is that of an infinite linear chain, which is lower than that of a finite linear chain. To assess possible

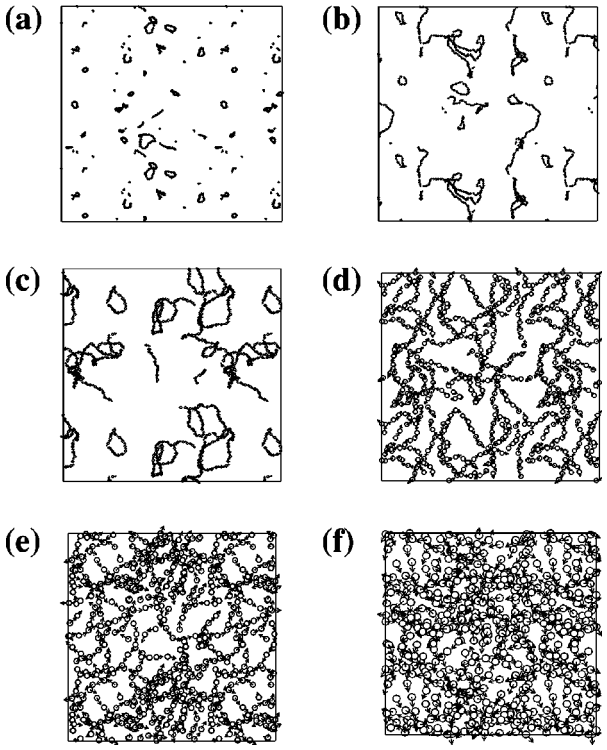

FIG. 1. Typical configurations from MC simulations of $N=256$ particles along the isotherm $T^*=0.1\dot{3}$, at various densities, ρ^*: (a) $\rho^*=0.001$, (b) $\rho^*=0.005$, (c) $\rho^*=0.01$, (d) $\rho^*=0.06$, (e) $\rho^*=0.17$, and (f) $\rho^*=0.35$.

simulation artifacts, we repeated the simulation at $\rho^*=0.01$ with a larger system size of $N=512$ particles. Extremely similar structure was observed, and the energies agree within statistical error, as shown in Table I.

At a density $\rho^*=0.06$ there is a distinct change in structure. Figure 1(d) shows that there are no ringlike clusters, but only relatively short chainlike segments that form a network of long chains, which extends throughout the simulation cell. It is now possible to trace a path along pairs of spheres at, or close to, contact, from one side of the cell to the other. It is unlikely that the periodic boundary conditions are strongly perturbing the ''true'' structure, however, since by inspection of Fig. 1(d), the structure is linear over length scales much less than the box length.

At higher densities the network structure of the fluid disintegrates until no significant association is apparent. Figures 1(e) and 1(f) show configurations at densities $\rho^*=0.17$ and $\rho^*=0.35$, respectively, that illustrate how the network structure is superseded by a more normal dense liquid structure, as the density is increased. For the sake of brevity, we only mention that configurations from the simulations with $\rho^*=0.5$ and $\rho^*=0.6$ show no unusual positional correlations, but only the alignment of the dipoles in the orientationally ordered liquid phase.

From Fig. 1, the following features of particle association in different regimes of density can be identified. The average cluster size appears to increase with increasing density, up to $\rho^*\simeq 0.06$. At low densities the free energy is dominated by entropy, which obviously favors a large number of small clusters. Indeed, if the density is low enough the fluid must be almost completely dissociated. As the density is increased the intracluster energy becomes increasingly significant, and this favors the formation of larger clusters since the neighboring dipoles in the cluster can more easily attain the nose-to-tail configuration. The decrease in entropy upon particle association is therefore compensated by the intracluster energy, and the average cluster size increases.

Another observation is that the proportion of ringlike clusters decreases as the density, and hence the typical cluster size, increase. Certainly the energy per particle of a ring of n particles is slightly lower than that of a chain of n particles, when $n\geqslant 4$, but the difference decreases as n increases. On the other hand, the entropy per particle of a chain is, presumably, higher than that of a ring. The differences in energy and entropy between those of an isolated chain and those of an isolated ring must be independent of density, and hence the observed unbinding of the rings to form chains as the density is increased is driven by interactions between different clusters. It would therefore appear that at low density ($\rho^*\leqslant 0.001$) the rings are stabilized by favorable *intracluster* interactions. As the density is increased the average cluster size increases; hence, when the rings unbind, they gain entropy, but do not lose a significant amount of binding energy. More importantly, there are greater opportunities for *intercluster* interactions afforded by having two ''dangling bonds'' per chain.

At densities in the region of $\rho^*=0.06$ there is clearly a high degree of connectivity between different chainlike segments, which results in a network that extends over the entire system. It is interesting that the fluid retains a roughly linear ordering of the dipoles within chainlike segments of up to about ten sphere diameters long. As the density is raised further, the network structure is destroyed, to be replaced by a more normal dense liquid structure, where each particle is no longer strongly associated with two nearest neighbors, but rather interacts with a whole coordination shell of near neighbors. As discussed in Ref. [16], this must result in an increase in the volume available to each particle, and hence to an increase in the excess entropy.

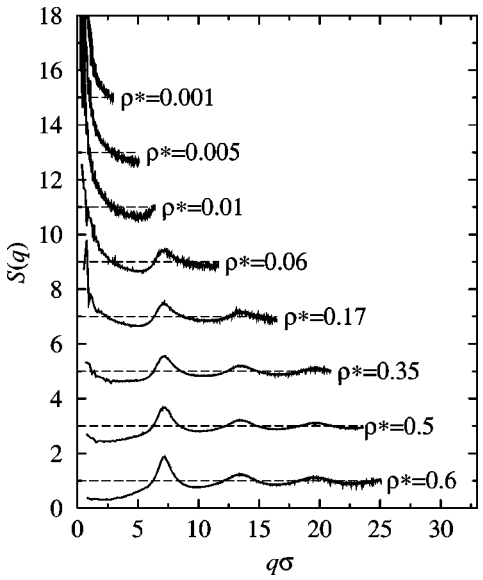

FIG. 2. The structure factor $S(q)$ as measured in MC simulations of $N=256$ particles along the isotherm $T^*=0.1\dot{3}$, at various densities ρ^*.

We now turn to the results for the static structure factor $S(q)$. In Fig. 2 we present $S(q)$ for each of the eight densities simulated. Note that the maximum available value of q increases with increasing density due to the fixed number of wave vectors used in the simulations. The peaks at $q\sigma\simeq 7$ and above are due to short-range correlations over distances of the order of a particle diameter; we would expect those peaks to be present at the lowest densities if enough wave vectors were included in the calculations. Weis and Levesque [12] remark that strong particle association leads to a slight asymmetry in these peaks. It is clear that the low-q region, up to $q\sigma\simeq 3$, contains the key differences between $S(q)$ at high and low density. At high density, $S(q)$ is almost constant as $q\to 0$, whereas at low density, $S(q)$ increases rapidly in the same limit. A result of classical statistical mechanics is that $S(0)=\chi_T/\chi_T^{\mathrm{id}}$, where χ_T is the compressibility of the fluid, and $\chi_T^{\mathrm{id}}=\beta/\rho$ is the compressibility of the ideal gas [26]. At high densities the spatial structure and thermodynamics are largely dictated by the hard cores, and hence the fluid is much less compressible than an ideal gas at the same number density. $S(0)$ should therefore be small at high density, and the results in Fig. 2 for $\rho^*=0.5$ and $\rho^*=0.6$ bear this out.

In Fig. 3, to highlight the low-q behavior of $S(q)$, we present the results on log-log plots, for all but the two highest densities. The region $q\sigma<1$ corresponds to the longest distances up to $L/2$, and hence $S(q)$ in this region must contain contributions from correlations between different clusters. Since there are very few distinct clusters in the simula-

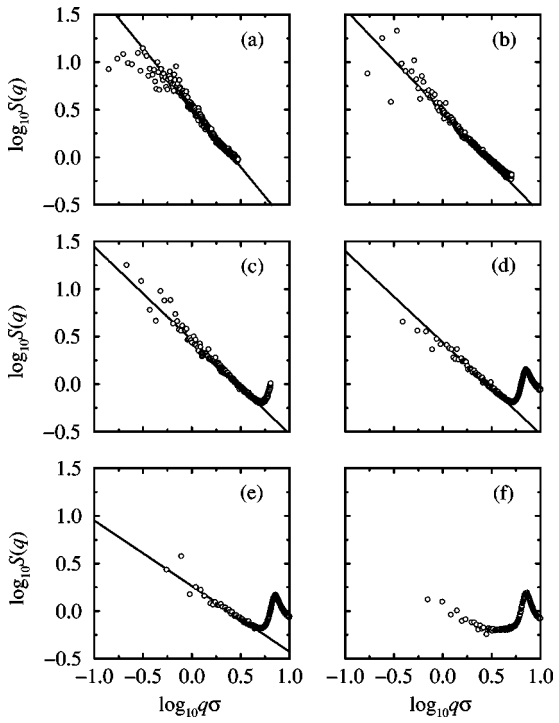

FIG. 3. Log-log plots of the structure factor $S(q)$ as measured in MC simulations of $N=256$ particles along the isotherm $T^*=0.1\dot{3}$, at various densities, ρ^*. (a) $\rho^*=0.001$, (b) $\rho^*=0.005$, (c) $\rho^*=0.01$, (d) $\rho^*=0.06$, (e) $\rho^*=0.17$, and (f) $\rho^*=0.35$.

tion, the statistics are poor. The situation is exacerbated by the fact that the number of wave vectors with magnitude q, decreases with decreasing q. For $\rho^* \leqslant 0.17$ there is clear power-law behavior in $S(q)$ in the range $1 \leqslant q\sigma \leqslant 3$.

The scaling of the structure factor in a given range of wave vectors can be related to the way in which the radial distribution function, $g(r)$, scales in the corresponding range of distances, $r \simeq 2\pi/q$ (see, e.g., Ref. [32]). The number of particles $N(r)$ within a distance r of a given particle, scales like $N(r) \sim r^D$. In general, D is the fractal dimension, which characterizes the structure on a particular length scale. The radial distribution function and structure factor in d dimensions therefore scale as

$$g(r) \propto \frac{1}{r^{d-1}} \frac{dN(r)}{dr} \sim r^{D-d}, \tag{5}$$

$$S(q) \sim q^{-D}, \tag{6}$$

where $D \leqslant d$. For rodlike molecules $D=1$, for a freely jointed polymer $D=2$, and for a random self-avoiding walk in three dimensions $D=5/3$.

For densities $\rho^* \leqslant 0.17$, $S(q)$ in the range $1 \leqslant q\sigma \leqslant \pi$ was fitted to the equation $S(q)=A(q\sigma)^{-D}$. This choice of upper limit on $q\sigma$ corresponds to a separation $r \simeq 2\sigma$. $S(q)$ for $q\sigma > \pi$ is dominated by correlations between adjacent particles at or close to contact. A fit to the data for $\rho^*=0.35$ was not attempted since there is clearly no significant scaling behavior. The fit parameters are reported in Table I, and the fitted curves are shown in Fig. 3. For densities in the range $0.005 \leqslant \rho^* \leqslant 0.06$, the parameter D is essentially equal to 1, which is indicative of chainlike spatial correlations. The structure factor measured in the 512-particle system at a density $\rho^*=0.01$ is omitted from Fig. 3 for clarity, but it is identical to that measured with $N=256$. The fit parameters for the two system sizes, shown in Table I, are also the same within the uncertainties associated with the fitting procedure. The value of D at $\rho^*=0.001$ is significantly greater than 1. From Fig. 1(a) we recall that the fluid at this density is largely made up of rings, rather than chains. For a perfectly circular, planar ring of particles, $N(r)$ should be roughly proportional to the portion of the ring within a distance r of any given particle in the ring. If the radius of the ring is R, and $r \leqslant 2R$, the result is $N(r) \propto 2R \arccos(1-r^2/2R^2) = 2r + r^3/12R^2 + \cdots$. Therefore, in the relevant range of wave vectors, we would expect the structure factor of ringlike clusters to behave like $S(q)=A/q+B/q^3+\cdots$, i.e., it increases faster than $1/q$. This is the reason why the measured parameter D is significantly greater than 1. At a density $\rho^*=0.17$, D is significantly less than 1, which is indicative of the transformation between the low-density associated structure, and the normal dense liquid structure.

In summary, we note that for all of the densities in the range $0.005 \leqslant \rho^* \leqslant 0.06$, $S(q)$ shows power-law behavior in the range $1 \leqslant q\sigma \leqslant \pi$. This suggests that the fluid structure in this regime is made up of a single basic building block, this being a rodlike segment of about six or seven particles arranged in an almost linear nose-to-tail configuration. The extent of such a segment can be thought of as a kind of persistence length, with the segments being associated further to form polymerlike chains and rings. This persistence length is similar in magnitude to that measured by Weis and Levesque [11,12]. These features are also apparent by inspection of the simulation configurations shown in Fig. 1. The crossover from an associated low-density structure to a more normal high-density liquid structure therefore seems to occur when the fluid can no longer accommodate a persistence length of about $6-7\sigma$.

IV. CONCLUSIONS

In this paper we have presented the results of extensive computer simulations of the DHS fluid at various densities along a single isotherm, below the estimated critical isotherm. Using a combination of computer graphics and calculations of the static structure factor, we have identified three regimes of particle association. At very low densities the fluid is made up of a mixture of rings, chains, and some free particles. As the density is increased the degree of association increases, and the rings unbind to form almost linear segments, of about six or seven particles, that connect to form an extended network. Further compression results in the destruction of this network, and the system crosses over to a more normal dense liquid phase. Since the persistence length of the clusters is significantly less than the box length of a 256-particle system at the densities of interest, we are confident that finite-size effects are small. We have provided an analysis of the structure factors at low wave vectors, which highlights the nature of particle association, and provides a means of discriminating between the low and high-density phases either side of the fluid-fluid transition.

The progression of structures in the DHS fluid upon compression is reminiscent of the behavior of some other

network-forming fluids. In a recent example, Katayama *et al.* [33] used synchrotron x-ray techniques to study a first-order liquid-liquid transition in phosphorus. In this case the transition is between a low-pressure molecular liquid, made up of tetrahedral P_4 units, and a high-pressure polymeric liquid. The phases were distinguished by the structure factor, with a linear combination of low-pressure and high-pressure functions being observed in the coexistence region. Although this transition is accompanied by electronic as well as structural rearrangements, it does illustrate how scattering experiments can be used to locate a first-order phase transition between fluids with distinct *local* structures.

To our knowledge the only ferrofluids which have been shown to exhibit a vapor-liquid transition are the so-called ionic ferrofluids [17,18]. The experimental techniques, which might prove appropriate to the study of low-density, strongly interacting ferrofluids, have been discussed by de Gennes and Pincus [2]. These include light scattering in thin films, microscopic observation, and small-angle x-ray scattering. It is our hope that scattering experiments can be performed on ferrofluids in which the particles possess a sufficiently large dipole moment to exhibit the anticipated vapor-liquid transition.

ACKNOWLEDGMENT

The financial support of the National Science and Engineering Research Council of Canada is gratefully acknowledged.

[1] P.H. Hess and P.H. Parker, Jr., J. Appl. Polym. Sci. **10**, 1915 (1966).
[2] P.G. de Gennes and P.A. Pincus, Phys. Kondens. Mater. **11**, 189 (1970).
[3] P.C. Jordan, Mol. Phys. **25**, 961 (1973).
[4] I. Jacobs and C. Bean, Phys. Rev. **100**, 1061 (1955).
[5] A.S. Clarke and G.N. Patey, J. Chem. Phys. **100**, 2213 (1994).
[6] H.B. Lavender, K.A. Iyer, and S.J. Singer, J. Chem. Phys. **101**, 7856 (1994).
[7] D. Lu and S.J. Singer, J. Chem. Phys. **103**, 1913 (1995).
[8] M.A. Osipov, P.I.C. Teixeira, and M.M. Telo da Gama, Phys. Rev. E **54**, 2597 (1996).
[9] J.M. Tavares, M.M. Telo da Gama, and M.A. Osipov, Phys. Rev. E **56**, R6252 (1997).
[10] J.M. Tavares, J.J. Weis, and M.M. Telo da Gama, Phys. Rev. E **59**, 4388 (1999).
[11] J.J. Weis and D. Levesque, Phys. Rev. Lett. **71**, 2729 (1993).
[12] D. Levesque and J.J. Weis, Phys. Rev. E **49**, 5131 (1994).
[13] We note that the definition of a cluster is somewhat subjective, and that a recent simulation study by Tavares *et al.* [10] shows that the resulting chain statistics are sensitive to the exact choice of criterion.
[14] J.M. Caillol, J. Chem. Phys. **98**, 9835 (1993).
[15] M.E. van Leeuwen and B. Smit, Phys. Rev. Lett. **71**, 3991 (1993).
[16] P.J. Camp, J.C. Shelley, and G.N. Patey, Phys. Rev. Lett. **84**, 115 (2000).
[17] J.-C. Bacri, R. Persynski, D. Salin, V. Cabuil, and R. Massart, J. Colloid Interface Sci. **132**, 43 (1989).
[18] E. Dubois, V. Cabuil, F. Boué, and R. Perzynski, J. Chem. Phys. **111**, 7147 (1999).
[19] D. Wei and G.N. Patey, Phys. Rev. Lett. **68**, 2043 (1992).
[20] D. Wei and G.N. Patey, Phys. Rev. A **46**, 7783 (1992).
[21] J.J. Weis and D. Levesque, Phys. Rev. E **48**, 3728 (1993).
[22] M.J. Stevens and G.S. Grest, Phys. Rev. E **51**, 5962 (1995).
[23] B.J. Costa Cabral, J. Chem. Phys. **112**, 4351 (2000).
[24] M.P. Allen and D.J. Tildesley, *Computer Simulation of Liquids* (Clarendon, Oxford, 1987).
[25] S.W. de Leeuw, J.W. Perram, and E.R. Smith, Proc. R. Soc. London, Ser. A **373**, 27 (1980).
[26] J.-P. Hansen and I.R. McDonald, *Theory of Simple Liquids* (Academic Press, London, 1986).
[27] C. Zannoni, in *The Molecular Physics of Liquid Crystals*, edited by G.R. Luckhurst and G.W. Gray (Academic Press, New York, 1979), Chap. 3, pp. 191–220.
[28] P.G. de Gennes, *The Physics of Liquid Crystals* (Clarendon Press, Oxford, 1974).
[29] R. Eppenga and D. Frenkel, Mol. Phys. **52**, 1303 (1984).
[30] G. Ayton, M.J.P. Gingras, and G.N. Patey, Phys. Rev. Lett. **75**, 2360 (1995).
[31] G. Ayton, M.J.P. Gingras, and G.N. Patey, Phys. Rev. E **56**, 562 (1997).
[32] P.M. Chaikin and T.C. Lubensky, *Principles of Condensed Matter Physics* (Cambridge University Press, Cambridge, 1995).
[33] Y. Katayama, T. Mizutani, W. Utsumi, O. Shimomura, M. Yamakata, and K. Funakoshi, Nature (London) **403**, 170 (2000).